Mechanisms for ENSO Phase Change in a Coupled GCM

ERIC GUILYARDI* AND PASCALE DELECLUSE

LODYC, Paris, France

SILVIO GUALDI AND ANTONIO NAVARRA

INGV, Bologna, Italy

(Manuscript received 8 October 2001, in final form 22 August 2002)

ABSTRACT

The mechanisms leading to El Niño onset and termination in the ECHAM4/OPA coupled GCM are assessed and compared to observations and existing ENSO paradigms. At the equator as well as off equator, the patterns and timing of modeled El Niño composites are in good agreement with those observed. Heat content of the west Pacific is confirmed as a precursor to ENSO phase change, and the present work emphasizes the role of its northern off-equator part [west North Pacific (WNP) region, 5°–15°N, 120°–170°E]. The associated heat content changes appear to be dominated by a local Ekman pumping (or forced Rossby waves) rather than the accumulation of remotely generated free Rossby waves, as proposed by many theories. The heat content decrease in the WNP region, which triggers El Niño termination, is due to the negative feedback of the atmospheric Gill's response to the increased equatorial SST in the east Pacific, in agreement with most paradigms (delayed, recharged, west Pacific oscillators). The present study introduces the advection of the off-equator signal to the equatorial waveguide by the mean currents of the western Pacific as an additional process. A similar feedback (with opposite sign) also seems to drive the modeled El Niño onset, favoring a too strong and regular biennial ENSO in the model. This is due to the stronger-than-observed Walker circulation that isolates the WNP region from other remote influences (like monsoons). The model also exhibits ''aborted'' ENSO events where the warming peaks in late spring instead of late autumn and is quickly terminated by the Gill's negative feedback. The abort event occurs too frequently in the coupled model due to too strong and too zonal a convergence zone south of the equator (''double ITCZ''). It bears some resemblance to the spring 1993 warming, when the southern Tropics were also warm. The results of this paper provide additional insight into the El Niño seasonal phase lock mechanisms.

1. Introduction

Since the work of Bjerknes (1969), the understanding of El Niño–Southern Oscillation (ENSO) has significantly increased [see the special issue of the *Journal of Geophysical Research* (1998, vol. 103, no. CC7)]. Many studies addressed ENSO phase change, a key issue for ENSO prediction (Wyrtki 1975, 1985; White et al. 1985; Zebiak and Cane 1987; Shopf and Suarez 1988, 1990; Zebiak 1989; Weisberg and Wang 1997; Picaut et al. 1996; Jin 1997a; Li 1997; Perigaud et al. 2000). The rise of an El Niño event requires a positive feedback while its decay requires a negative feedback. While the former was more or less already described by Bjerknes (1969), the negative feedback that would terminate an event generated a large body of work. Based on either observational analysis or theoretical models several paradigms have been proposed. The delayed oscillator (Shopf and Suarez 1988; Battisti and Hirst 1989) depends upon a delayed negative feedback involving the reflection of ocean equatorial waves at the western boundary, these waves being generated by the atmosphere response to increased SST [the Gill's response described by Gill (1980)] in the east and central Pacific. The recharged oscillator (Jin 1997a) involves a similar process, but in the integral sense. The west Pacific oscillator (Weisberg and Wang 1997) involves a local negative feedback mechanism through the large-scale atmospheric response to increased SST. The advective–reflective oscillator (Picaut et al. 1996) emphasizes the importance of zonal advection and the reflection at both eastern and western boundaries. Attempts to classify (slow and fast modes; Neelin et al. 1998) and unify (Wang 2001) these paradigms were conducted, suggesting that depending on the process(es) neglected, a

* Current affiliation: Center for Global Atmospheric Modelling, Department of Meteorology, University of Reading, Reading, United Kingdom.

Corresponding author address: Dr. Eric Guilyardi, Center for Global Atmospheric Modelling, Department of Meteorology, University of Reading, Reading RG6 6BB, United Kingdom.
E-mail: ericg@met.rdg.ac.uk

paradigm may or may not become dominant. Moreover, the unequal skill of ENSO prediction models generated a debate on the relative importance of the processes included in these paradigms (e.g., the role of boundary wave reflection). Likewise, other processes are being considered as possibly important, while not explicitly part of the accepted ENSO paradigms. For example, studies stress the possible role of intraseasonal oscillations (Zhang et al. 2001) or nonlinear processes (Boulanger et al. 2002, manuscript submitted to *Geophys. Res. Lett.*).

If the diversity of events associated with a lack of detailed observed data has so far prevented the description of a single robust mechanism for ENSO turnabout (if existing), most theories emphasize the role of the west Pacific heat content as a precursor to ENSO phase change. This role was anticipated by several early works (the ''recharge'' of Wyrtki 1975, 1985; White et al. 1985; Zebiak and Cane 1987) and theories (Shopf and Suarez 1988; Battisti and Hirst 1989; Weisberg and Wang 1997), and has since been demonstrated by several studies (Jin 1997a; Li 1997; Vintzileos et al. 1999; Wang et al. 1999; Cassou and Perigaud 2000; Meinen and McPhaden 2001). The ENSO cycle is characterized by large-scale three-dimensional changes in the distribution of upper-ocean and atmospheric heat and mass in the tropical Pacific. The exchanges between the equatorial waveguide and off-equator[1] regions therefore play a key role in the behavior of ENSO. These studies broadly showed that the mean zonal equatorial thermocline contains the memory carried over between ENSO events (Li 1997; Jin and An 1999; Collins 2000; Meinen and McPhaden 2001), and the associated depth variations are fed by changes in the off-equator heat content. From recent ocean analysis [the National Centers for Environmental Prediction (NCEP) ocean reanalysis—Ji et al. 1995 and Levitus and Boyer 1994], Wang et al. (1999) and Zhang and Levitus (1996) have shown that during most ENSO cycles heat content anomalies in the west Pacific had wide meridional structures and that most were initiated off equator.

If this off-equatorial role is now well agreed upon, the mechanisms that modify the heat content in the west Pacific at these latitudes are still unclear. Several mechanisms have been proposed, keeping in mind that the SST varies very little in this region and cannot explain the magnitude of the local atmospheric response as in the east and central Pacific. Based on the analysis of the Zebiak and Cane (1987) model, Jin (1997b) and Cassou and Perigaud (2000) describe a basinwide Sverdrup balance adjustment; Schopf and Suarez (1990) and Li (1997) put forward an accumulated effect of oceanic waves and their reflection at the western boundary; Zhang et al. (1998) propose the subduction of midlatitude waters to lower latitudes; Weisberg and Wang (1997) and Wang et al. (1999) explain the change of the off-equatorial heat content by the impact of local wind forcing (through Ekman pumping) due to a modified large-scale atmospheric circulation; Zhang and Rothstein (2000) emphasize equatorward Ekman convergence in the central Pacific; and, based on reconstructed datasets, Meinen and McPhaden (2001) emphasize net meridional transport south of the equator.

The transport of these off-equator heat content anomalies to the equatorial waveguide is briefly discussed in these studies. Nevertheless, this transport most likely involves a delay that is important for ENSO phase change. More work is needed to describe the processes involved (wave propagation or ocean advection).

Simplified anomaly models were instrumental in clarifying basic ENSO dynamics. Nevertheless, they omit important processes. For instance, their assessment of off-equator processes and more remote effects is still incomplete (Perigaud et al. 2000). Likewise, the role of the annual cycle is briefly discussed in ENSO paradigms, even though there is ample evidence that the evolution of ENSO is strongly linked with the seasons (Rasmusson and Carpenter 1982; Wang 1994), especially during El Niño onset and decay. This may be due to the fact most of the simple coupled models specify the annual cycle and forecast anomalies. They, thus, essentially break the linkage between the annual cycle and the interannual variability. The hypothesis drawn from the analysis of these simplified models must therefore be confirmed with more comprehensive climate models, that is, GCMs. Most present-day coupled ocean–atmosphere GCMs claim ENSO-like variability. The performance of these models has clearly improved over the years (Mechoso et al. 1995; Delecluse et al. 1998; Covey et al. 2000; Latif et al. 2001; AchutaRao and Sperber 2002), and the assessment can now go beyond the classic statistical and descriptive analysis and involve more process-based assessments (Raynaud et al. 2000). The high-quality direct observations available for the 1997/98 ENSO event [both in space and in time thanks to the TOPEX/Poseidon and the European Remote Sensing (ERS) satellites and the Tropical Atmosphere Ocean (TAO) moored array] provide an unprecedented opportunity to assess in more detail the ENSO mechanisms at work. It thus provides a useful benchmark for GCMs.

In this study, we compare a state-of-the-art coupled ocean–atmosphere GCM, typical of those recently being used for ENSO prediction, and observations in order to analyze 1) which mechanisms lead to off-equator heat content anomalies in the west Pacific, 2) how do these anomalies reach the equatorial waveguide, 3) how this feeds into large-scale ENSO phase change feedbacks, and 4) how these compare with ENSO paradigms.

The coupled model is presented in section 2. Section 3 presents a tropical validation leading to the analysis of the model ENSO composites. Section 4 examines in

[1] In this study, ''off-equator'' refers to tropical regions outside the equatorial waveguide, that is, unless otherwise specified, between 5° and 15°N and between 5° and 15°S.

more detail the mechanisms for El Niño's decay and onset in the model. A summary and concluding remarks follow in section 5.

2. The SINTEX coupled model

The model used for this study is the ECHAM–ORCA coupled GCM developed within the Scale Interaction Experiment (SINTEX) European Union project.

a. The ORCA model

ORCA is the global version of the Océan Parallélisé (OPA) 8.1 ocean modeling system developed by the Laboratoire d'Océanographic Dynamique et de Climatologie (LODYC) team in Paris (Madec et al. 1998, more information available online at http://www.lodyc.jussieu.fr/opa/). It is a finite-difference OGCM and solves the primitive equations with a nonlinear equation of state on a C grid. The present configuration uses a rigid lid. The horizontal mesh is orthogonal and curvilinear on the sphere. It does not have a geographical configuration: to overcome the singularity at the North Pole, the northern point of convergence has been replaced by two poles located on Asia and North America. Its space resolution is roughly equivalent to a geographical mesh of $2° \times 1.5°$ (with a meridional resolution of 0.5° near the equator). Thirty-one vertical levels are used with 10 levels in the top 100 m. Vertical eddy diffusivity and viscosity coefficients are computed from a 1.5 turbulent closure scheme that allows an explicit formulation of the mixed layer as well as minimum diffusion in the thermocline (Blanke and Delecluse 1993). Horizontal mixing of momentum is of the Laplacian type with an eddy viscosity coefficient of 40 000 $m^2\ s^{-1}$, reduced in the Tropics to reach 2000 $m^2\ s^{-1}$ at the equator. The lateral mixing of tracers (temperature and salinity) is ''quasi-pure'' isopycnal as described by Guilyardi et al. (2001). This model has been extensively validated in an uncoupled mode in the Tropics where its close agreement with observations was shown by Vialard et al. (2001). ORCA is also widely used in the coupled mode for process studies (Guilyardi et al. 2001; Raynaud et al. 2000; Inness et al. 2003), paleoclimate simulations (Braconnot et al. 1999), and climate change experiments (Barthelet et al. 1998; Friedlingstein et al. 2001). There is no interactive sea ice model in the configuration used for the present tropical study: the sea ice cover is relaxed toward observed monthly climatology.

b. The ECHAM4 model

ECHAM4 is the fourth generation of the ECHAM atmospheric general circulation model (AGCM) developed at the Max-Planck-Institut Für Meteorologie in Hamburg, Germany. ECHAM is an evolution of the spectral numerical weather prediction model developed at the European Centre for Medium-Range Weather Forecasts (ECMWF), but significantly modified to make it suitable for climate studies. In the successive model generations, several parameterization schemes were either replaced or additionally implemented. An exhaustive and detailed description of the dynamical and physical structure, and the simulated climatology of ECHAM4 has been given by Roeckner et al. (1996). Here we briefly summarize the main characteristics of the model. The prognostic variables in ECHAM4 include vorticity, divergence, temperature, surface pressure, water vapor, and cloud water. The model equations are solved on 19 hybrid vertical levels (top at 10 hPa) by using the spectral transform method with triangular truncation at wavenumber 30 (T30). Nonlinear terms and physical processes are computed on a Gaussian grid, providing a resolution of approximately 3.75° in longitude and latitude. ECHAM4 uses a semi-Lagrangian transport method for the advection of cloud water and water vapor (Rasch and Williamson 1990). The parameterization of convection is based on the mass flux concept, where cumulus clouds are represented by a bulk model including the effects of entrainment and detrainment on the updraft and downdraft convective mass fluxes (Tiedtke 1989). According to Nordeng (1994), the organized entrainment and detrainment are related to buoyancy, and an adjusted-type closure based on convective available potential energy (CAPE) is used. The radiation code is the same as Morcrette (1991) with a few modifications such as the inclusion of additional greenhouse gases, revised parameterization for the water vapor continuum and for the cloud optical properties.

c. Coupling procedure and initialization

ORCA and ECHAM4 are coupled through the Ocean Atmosphere Sea Ice and Soil (OASIS) coupler version 2.4 (Valcke et al. 2000). The coupling strategy is similar to that of Guilyardi et al. (2001). From Levitus (1982), the model is integrated for 2 yr in ocean robust-diagnostic mode. Once the ocean currents are spun up, the integration continues without any adjustment or restoring (except in regions where sea ice cover does not agree with climatology). Air–sea fluxes and SST are exchanged every 3 h. The simulation analyzed in this study was integrated for 200 yr.

3. Tropical validation

The global validation of the coupled model is beyond the scope of the present study. Other studies using the same simulation to document other climatic features help give a general overview (Gualdi et al. 2002a,b). It is worthwhile to note the absence of any rapid (1–5 yr) drift for most of the air–sea interface. The model is balanced: the radiative budget at the top of the atmosphere is close to zero and stays so for the 200 yr. Some

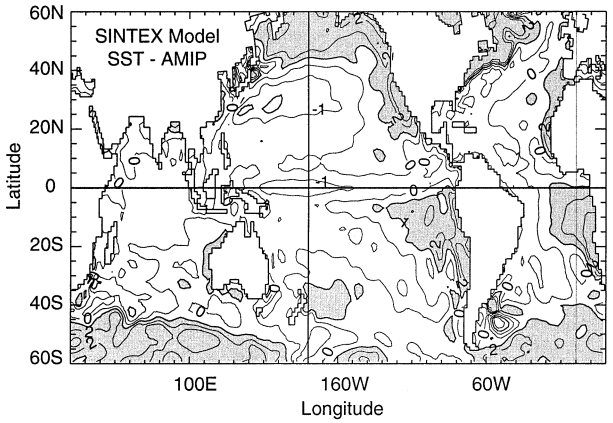

FIG. 1. SST errors of the SINTEX ECHAM4–ORCA coupled simulation, [difference with Atmospheric Model Intercomparison Project 2 (AMIP2) climatology]. Contour interval is 1°C. Light shading indicates cooling, dark shading indicates warming.

localized drifts appear at high latitude due to salinity errors associated with the lack of interactive sea ice.

a. Mean state

In the Tropics, the SST does not fall into a warm or a cold state (Fig. 1), as often seen in coupled GCMs that are not flux-corrected (Mechoso et al. 1995; Covey et al. 2000; Latif et al. 2001). The classic warming in the subtropical eastern ocean basin is present (Fig. 1), most likely due to the classic lack of low marine stratocumulus clouds (Mechoso et al. 1995; Terray 1998). A slight cooling appears around the equator in the central Pacific, due to stronger-than-observed trade winds (Fig. 2). These intensified trade winds are active all year-round but the difference is the strongest in March, when the model fails to reproduce the observed spring relaxation of the equatorial trades (Fig. 2a). This too active Walker circulation reduces the eastern extent of the equatorial warm pool by about 20° of longitude. In northern spring, the model develops a southern convergence zone (SCZ) centered at 10°S (Fig. 2a). This bias is the result of a too strong South Pacific convergence zone (SPCZ), its eastern extent being shifted toward the equator. This SCZ behaves like a southern ITCZ and such a symmetrization of the circulation is often seen in coupled GCMs using a spectral AGCM (Guilyardi and Madec 1997; Meehl and Arblaster 1998). In the present model, the northern ITCZ in autumn is captured quite well (Fig. 2b).

The equatorial thermocline slope and structure, which are important for ENSO dynamics, are well reproduced by the coupled model (Fig. 3). The warm pool is eroded and the thermocline is a bit too deep in the central Pacific, both features due to the strong trades. Other equatorial features (including zonal current and upwelling) broadly agree with the ones validated by Vialard et al. (2001) against Tropical Atmosphere Ocean (TAO)/Triangle Trans-Ocean Buoy Network (TRITON) array data (not shown).

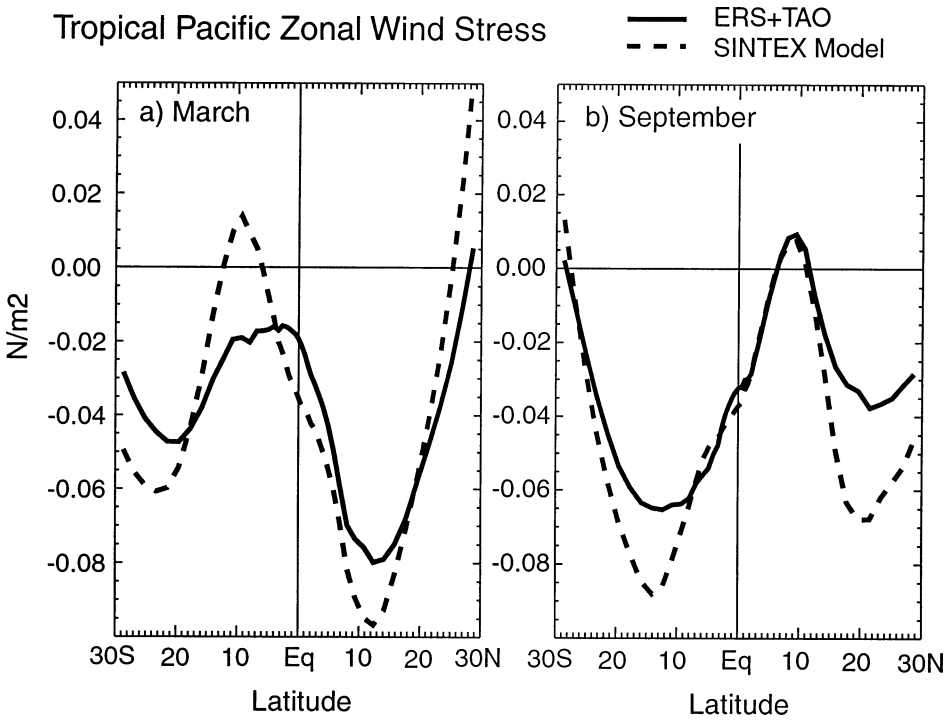

FIG. 2. Zonal wind stress in the tropical Pacific: (a) Mar, (b) Sep. Solid line is the ERS climatology corrected by observed TAO winds (Vialard et al. 2001). Dashed line is the SINTEX coupled model.

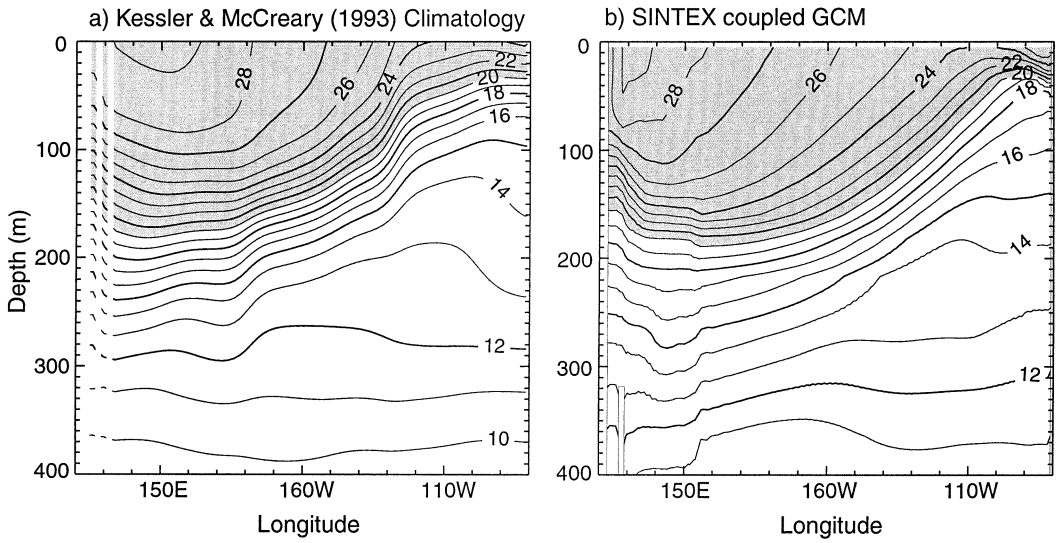

FIG. 3. Annual mean temperature section at the equator: (a) Kessler climatology (Kessler and McCreary 1993), (b) SINTEX coupled model. Contour interval is 1°C. Shading indicates temperatures above 20°C.

b. Interannual variability

A detailed assessment of tropical variability statistics is given by Gualdi et al. (2002b). Here, we use the Niño-3 (5°N–5°S, 90°–150°W) SST anomaly to select individual events and build their composites. The modeled Niño-3 SST anomaly exhibits a variability slightly weaker than the Hadley Centre Global Sea Ice and Sea Surface Temperature (HadISST) 1.1 SST dataset (N. Rayner et al. 2002, personal communication; standard deviation of 0.6° compared to 0.8°C for observations; Fig. 4). Most of the modeled variability is within 1.5 standard deviations, a feature also observed until the 1970s. The Niño-3 SST anomaly spectrum shows an emphasized 2-yr peak and a weak variability at lower frequency when compared to observations (Fig. 5). A superimposition of all the modeled events warmer than 1.5 standard deviations (Fig. 6a) exhibits two types of events: a *regular* ENSO type where the Niño-3 warming starts in May, peaks in December, and terminates the following May (Fig. 6b); and an *aborted* ENSO type where the warming reaches a peak value in May and then abruptly decreases to reach a cold state a year later (Fig. 6c). The first type is reminiscent of the observed ENSO and will be assessed in the following section. The second type appears to be a model bias, as such a behavior is not frequently seen in observations (except for the unusual 1993 warming, as discussed later). Composites of both types (regular ENSO: 25 cases, and aborted ENSO: 10 cases) are made for the 3 yr encompassing the warming. In the following text, the ''previous year'' (year −1 for the model and 1996 for observations) is the onset year, the ''warming year'' (year 0 or 1997) is the year of mature events and the ''year after'' (year +1 or 1998) is the decay year, as also defined by Rasmusson and Carpenter (1982). Following the method of Terray et al. (2003, manuscript submitted to *Climate Dyn.*), the significance of the composites were computed. Only the features that are significant at the 95% level are discussed in this study.

c. Model ENSO composite versus 1997/98 El Niño

The 1997/98 El Niño event has the basic features of most events since they have been observed with some degree of accuracy (McPhaden 1999), but for its intensity. Because of the unprecedented collection of high-quality measurements of this event, especially off equator, we choose it to validate the coupled model ENSO composite. The observed datasets are based on HadISST1 for the SST, ERS satellite winds corrected by TAO array local winds (Menkes et al. 1998), and TOPEX/Poseidon for the sea level.

The time–longitude sections of equatorial anomalies of SST, zonal wind, and heat content (or sea level) are presented in Fig. 7 for both the 1997/98 event and the model ENSO composite. In 1996, the equatorial SST in the western Pacific is slightly warmer than usual and slightly colder in the east (Fig. 7a), due to the stronger easterlies present there (Fig. 7b). The heat content, well correlated with the sea level, is already high in the western Pacific (Fig. 7c). These warm waters eventually cross the basin in successive Kelvin waves in early 1997, and, upon reaching the eastern boundary, trigger the SST warming (Fig. 7a). Due to the well-described ocean–atmosphere SST–wind feedback (Bjerknes 1969) the warming is further amplified in the central and eastern Pacific with a peak value reached in December 1997, as the westerly wind anomalies invade the central Pacific (Figs. 7a,b). Concurrently, the heat content in the western Pacific is reduced (Fig. 7c) and the corresponding

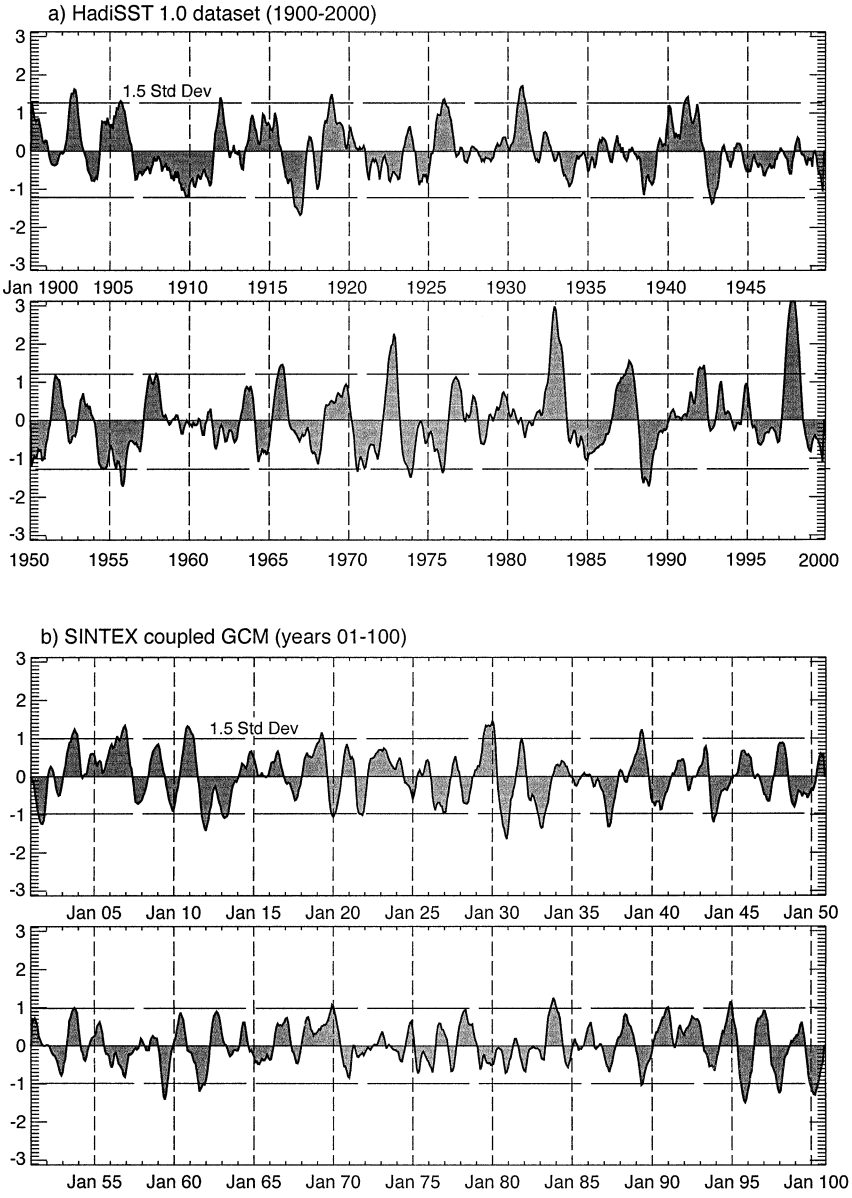

FIG. 4. Monthly Niño-3 SST anomaly time series. (a) HadISST1 observations for 1900–99. (b) SINTEX model for years 01–100. The ±1.5 std dev lines are indicated.

anomaly migrates eastward in early 1998, accompanying the termination of the event and leading to cold SST conditions in the central and eastern Pacific (Fig. 7a). These equatorial phases (and the elements specific to this particular event) are described in greater details by McPhaden (1999) and Vialard et al. (2001).

The model composite ENSO correctly exhibits many of the observed features of the 1997/98 event, both in spatial patterns and in timing (Figs. 7d–f). Together with simulating the correct seasonal cycle and mean state, this represent an important challenge for fully coupled GCMs without flux correction (Latif et al. 2001; AchutaRao and Sperber 2002). In particular, the subsurface anomalies also originate from the western Pacific (Fig. 7f) and propagate to the east as Kelvin waves in the beginning of the year (January–March), leading to SST changes in the eastern Pacific (Fig. 7d) and to the central Pacific invasion by westerly anomalies (Fig. 7e). Several differences can be seen. First, the amplitude of the signal is weaker in the model and the patterns are smoother, as expected from the averaging made to build the composite and the exceptional intensity of the 1997/98 event. The SST anomalies extend farther west in the model by 20°–30° of longitude (Fig. 7d), consistent with the stronger-than-observed Walker circulation. The cold SSTs in the central-eastern Pacific in the year prior to the event (and the associated increased easterlies) are relatively stronger than in observations. Apart

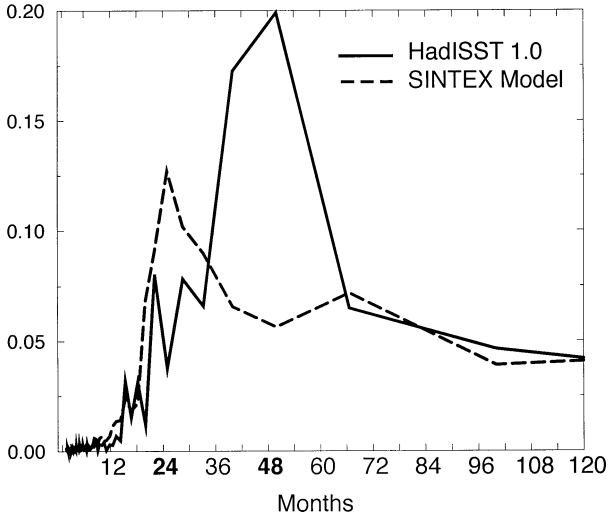

FIG. 5. Niño-3 SST anomaly spectrum. Solid line is the HadISST1 observations, and dashed line is the SINTEX coupled model. The time series were normalized by their respective std dev prior to spectrum computation.

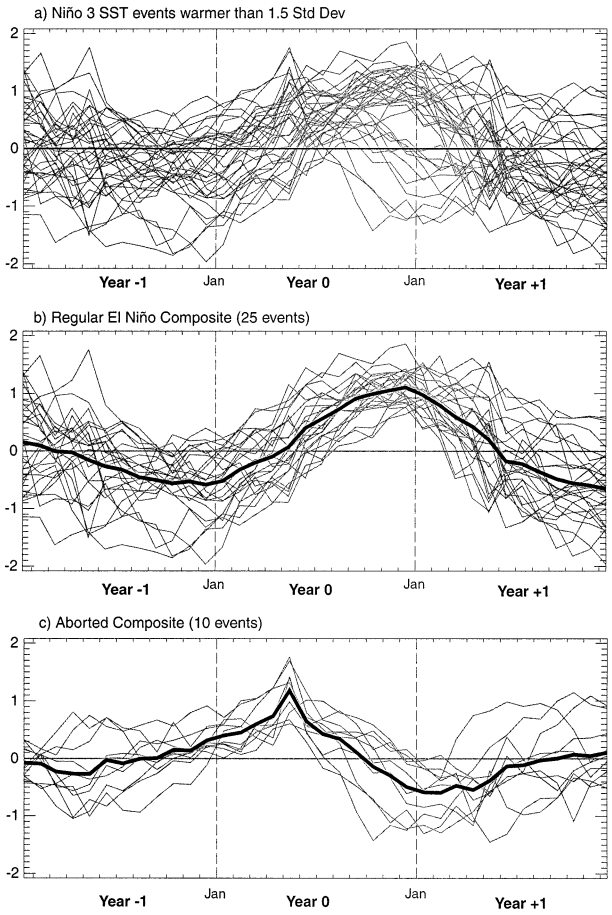

FIG. 6. (a) Superposition of Niño-3 SST anomalies for El Niño events warmer than 1.5 std dev, (b) regular ENSO-type subset (25 cases), (c) aborted ENSO-type subset (10 cases). The thick curves represent the composite mean of each type.

from these differences, the agreement between the model and the observations is evidence for correct ocean–atmosphere equatorial dynamics simulation in the SINTEX coupled model.

One of the major breakthroughs in ENSO observation was the launch of the TOPEX/Poseidon satellite, which gave coherent space and time sea level patterns for the 1997/98 El Niño, the first large event since its launch. The corresponding sequence of sea level anomalies is given every 3 months in Fig. 8a. The zonal evolution of heat content at the equator described in Fig. 7c is also visible here. The transfer of heat content anomalies from the west to the east occurs abruptly between February and May. These anomalies originate from the west of the basin, and in particular from the west North Pacific region (WNP; 5°–15°N, 120°–170°E), as seen in August and November of 1996 (warming) and of 1997 (cooling; note that the signal for the cooling in 1997 is clearer). Wang et al. (1999) describe the same WNP origin of heat content anomalies (for the 1982 and 1987 El Niño ''long cycle'' events, their Fig. 4) from the Ji et al. (1995) ocean analysis based on in situ data. Based on the annual average, Zhang and Levitus (1996) describe similar features. These patterns agree with many other studies, which have suggested that a buildup of warm waters in the western Pacific was a necessary precondition to the development of El Niño. The poleward heat discharge in observations is located in the eastern Pacific during several months of peak warming in the eastern Pacific (again similar to the Wang et al. 1999 long cycle composite).

The coupled model ENSO composite heat content anomaly exhibits the same structures and timing as in the observations (Fig. 8b). An off-equator recharge of the WNP region is also occurring during the second part of the year (August–December), both for the warming stage (year −1) and for the cooling stage (year 0). The anomalous heat content generated in the western Pacific is then transferred to the east along the equator, between February and May (as already seen in Fig. 7f). Finally, the heat is removed poleward from the eastern Pacific through both coastal Kelvin waves and interior transport (Fig. 8b). These maps also show that the anomalous zonal extent of the cold tongue in the model is confined to the equator.

The zonal mean heat content of the equatorial Pacific in the model composite leads the peak of ENSO by 8–10 months (Fig. 9). This confirms that zonal mean thermocline depth variation is a precursor to El Niño development, as also shown by Zebiak (1989, his Fig. 2) and Li (1997, his Fig. 3b). These depth variations are mostly due to the western Pacific and further analysis is needed to describe their origin.

4. Mechanisms for ENSO phase change

Both in the model and in observations, the heat content change of the western Pacific first appears in the

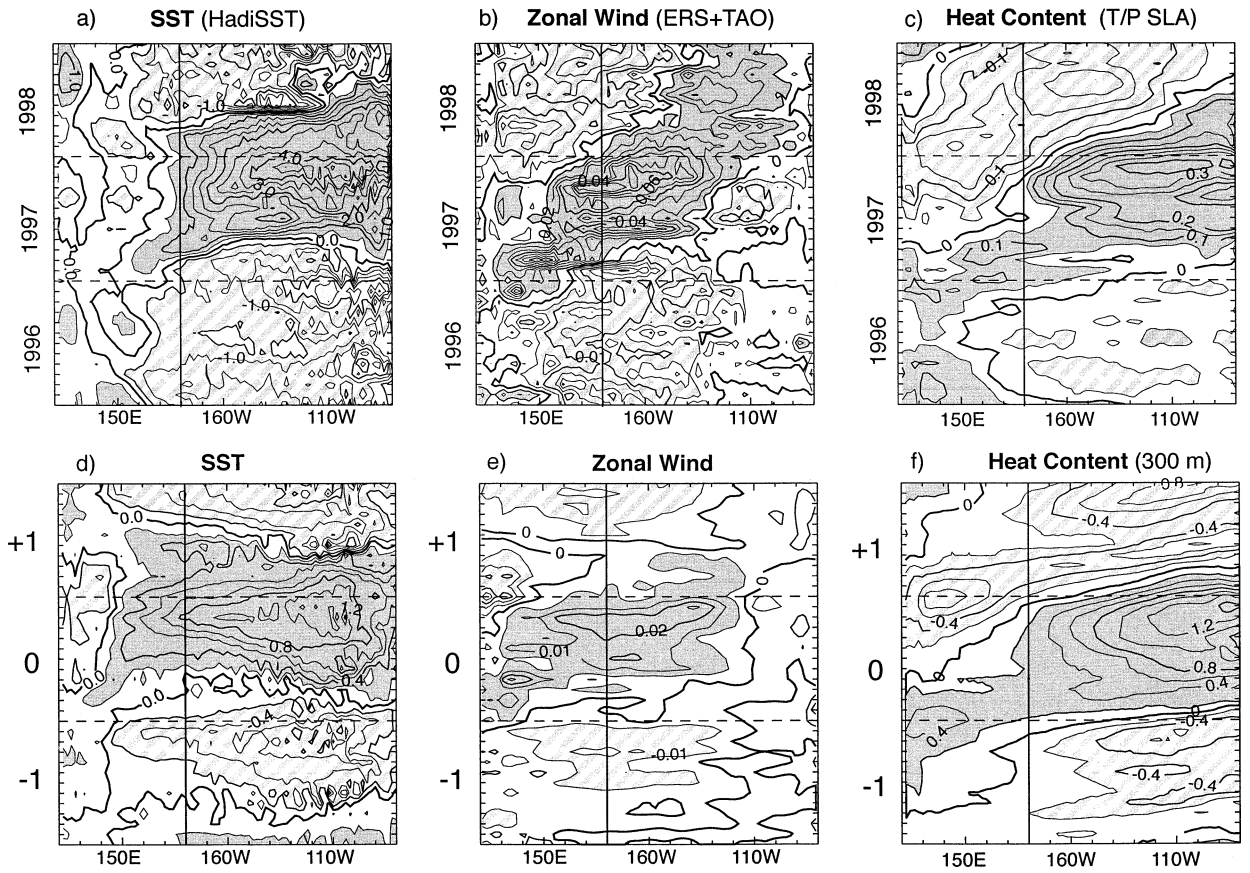

FIG. 7. Time–longitude diagrams of monthly equatorial anomalies of (a),(d) SST; (b),(e) zonal wind; (c) sea-level, and (f) heat content. The 1997/98 observations (HadISST1, ERS + TAO, TOPEX/Poseidon) are shown in (a)–(c). Coupled model ENSO composite values are shown in (d)–(f). Note the different contour intervals: (a) 0.5°C, (b),(e) 0.01 N m^{-2}, (c) m, (d) 0.1°C, (f) 0.2 GJ m^{-2}.

WNP region (Fig. 8). If the WNP area appears to be the initial location for ENSO phase change, several questions remain to fully describe the ENSO turnabout in the model. First, how does heat accumulate or diminish in the WNP region? Second, how are the associated anomalies transferred to the equator? And third, how do the mechanisms involved fit into the larger-scale feedback loops proposed by theories?

Two types of mechanisms have been proposed to explain the WNP heat content change: 1) an accumulated effect of off-equator remotely forced free Rossby waves (Li 1997; Perigaud et al. 2000), or 2) a local Ekman pumping via the local wind field (Weisberg and Wang 1997; Wang et al. 1999). This last process is also referred to as forced Rossby waves in several studies (Schopf and Suarez 1990). In support of the second mechanism, Wang et al. (1999) showed that the tendency of thermocline displacement in the WNP region and the local wind stress curl exhibit a coherent, broad spectral peak on an 8–20-month timescale. In order to estimate the contribution of local Ekman pumping to the anomalous heat content, a time–longitude section of heat content anomalies and a 6-month running time integral of the wind stress curl meridionally averaged between 5° and 15°N was performed for both the model and observations. The resulting figure (Fig. 10) suggests that the local wind forcing is dominant in both the observations and the model and explains a large part of the heat content/sea level signal. From spring to autumn 1997 (year 0), the positive wind stress curl in WNP (Figs. 10b,d) contributes to a shallowing of the thermocline through Ekman pumping: the heat content decreases and the sea level lowers (Figs. 10a,c). The reverse mechanism is seen in 1996 (year −1), although the signal is weaker, especially in the observations. If there is an influence of off-equatorial free Rossby waves (which should appear as a westward-propagating signal), it seems to be of secondary importance in the onset and termination of ENSO (Zebiak 1989; Graham and White 1991). They probably influence the long-term adjustment of the western Pacific, together with subduction from higher latitudes (Zhang et al. 1998) and other slow processes of low amplitude that contribute to the preconditioning of this key region (Schneider et al. 1999). Nevertheless, more detailed calculations in the ocean would be needed to prove this point. Moreover, the relative importance of free and forced Rossby waves could vary with each event. Finally, the west

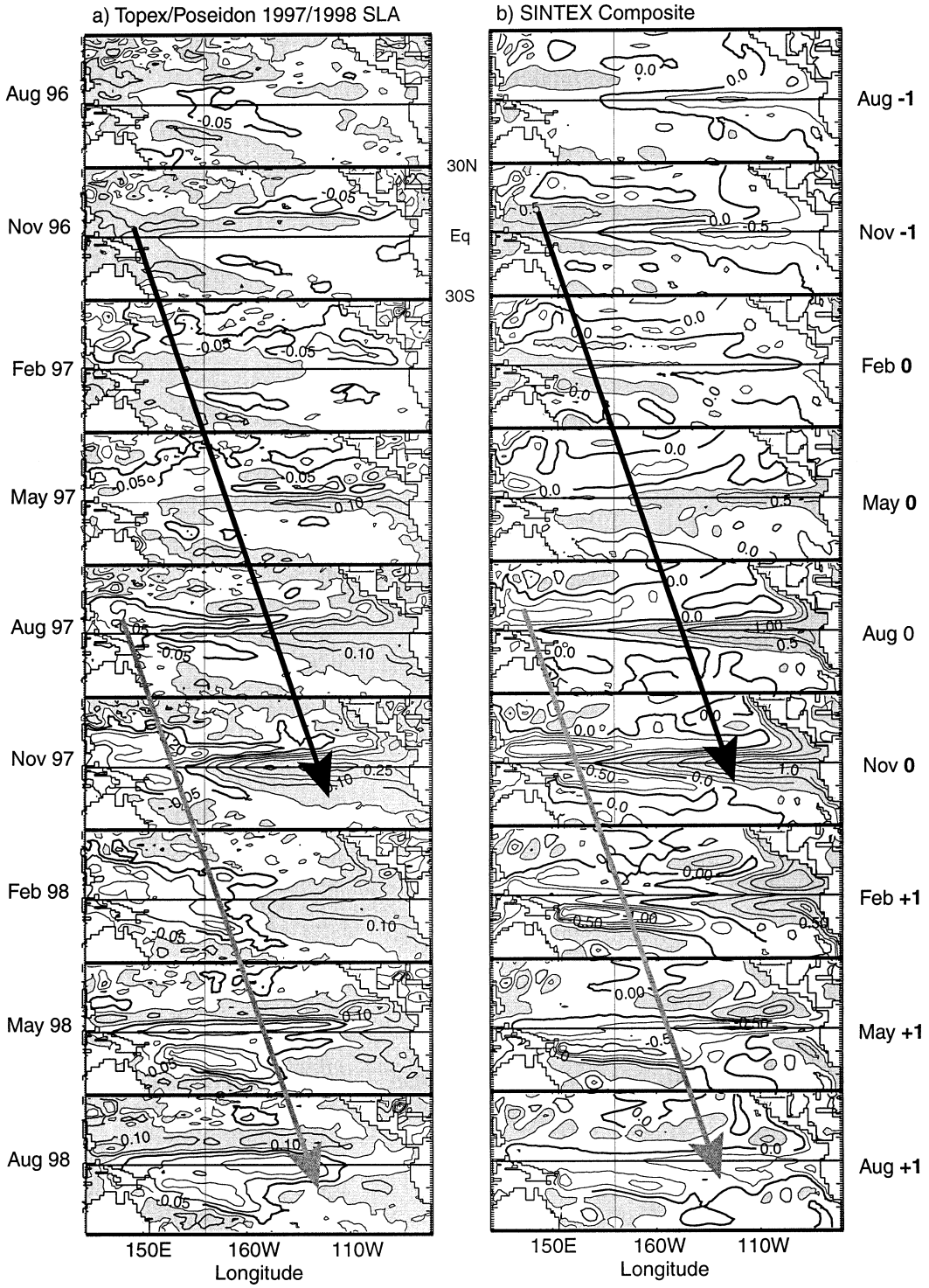

FIG. 8. (a) The 1997/98 El Niño cycle of sea level anomalies in the tropical Pacific from TOPEX/Poseidon. (b) Heat content anomalies for ENSO composite cycle in SINTEX coupled model. Time interval is 3 months. Shading indicates increased heat content. The dark (light) arrows represent the propagation of positive (negative) heat content anomalies.

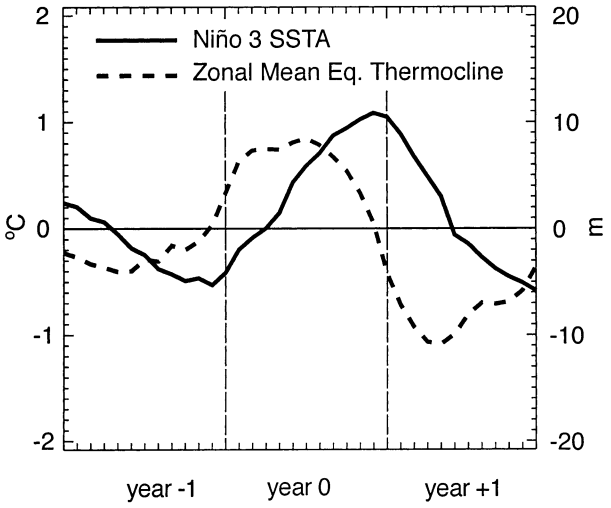

FIG. 9. Time series of (solid) Niño-3 SST anomaly and (dashed) zonal mean thermocline depth (averaged between 2°N and 2°S) for the 3-yr model ENSO composite. Thermocline depth is divided by 10.

Pacific model errors (equatorial easterly bias) might imply less obvious propagation of free Rossby waves (even though the bias becomes small off equator).

a. El Niño termination

We first assess the ENSO turnabout from warm El Niño conditions to normal/cold conditions, as the corresponding signal is strong both in the observations and in the model (Figs. 8 and 10). A time–latitude section of heat content anomalies zonally averaged over the western Pacific (120°N–170°E) for observations and for the model ENSO composite is presented in Figs. 11a,c. The off-equatorial initiation of the anomalies (in the north) and their subsequent equatorward propagation is seen both in the observations and in the model (Figs. 11a,c). The 6-month running time integral of the wind stress curl (Figs. 11b,d) is also well correlated with the off-equatorial heat content anomalies, strengthening the case of the local effect of the wind pumping as a dominant mechanism. This is even clearer for the negative heat content anomaly rising in the second half of the warming year (1997, year 0) between 5° and 15°N (Figs. 11a,c). In the Southern Hemisphere, the wind stress curl changes sign, but as the Coriolis parameter also changes sign, the Ekman pumping remains of the same sign, as seen in the winter months (note that the amplitude is weaker). These wind pattern changes are related to the large-scale atmosphere anomalous circulation due to the modified SST (Gill's response). Based on the evolution of the eastern Pacific SST (given by the normalized Niño-3 SST anomalies curves in Figs. 11b,d), this suggests the following negative feedback loop for El Niño termination: accompanying the SST warming in the eastern Pacific (during the warming year: 1997 or year 0), the atmospheric Gill's response generates a cyclonic wind stress anomaly between 5° and 15°N (Figs. 11b,d). The ocean integrates the corresponding anomalous Ekman pumping for several months (Figs. 11a,c). Near the end of the warming year, the associated anomalous heat content generated off equator is advected to the equator by the low-latitude current system of the western Pacific (see below). It is further transported to the eastern Pacific at the beginning of following year by equatorial Kelvin waves, as described previously, which cools the equatorial eastern Pacific, eventually leading to colder-than-normal SST in the second half of the following year (Figs. 11b,d). The lag necessary to a full development of the anomalous SSTs in the eastern Pacific is due to the following: 1) the time needed for the ocean to integrate the anomalous atmospheric forcing in WNP (6–8 months), 2) the time necessary for the off-equator ocean anomalies to be advected to the equator (~2 months), and 3) the time needed for the equatorial anomalies to propagate to the east (another 2 months), leading to the observed total lag of about a year (spring to spring).

This negative feedback loop evidenced in the model and validated by observations is mostly coherent with the several ENSO paradigms (delayed, recharged, or west Pacific oscillators). It supports the mechanism of west Pacific off-equator heat content change by local wind stress rather than the accumulation of free Rossby waves originating from the east Pacific. It also suggests that the northern west Pacific has a stronger role than the southern west Pacific. The time delay of one year computed above is in line with the one proposed by Suarez and Schopf (1988), except for the lag necessary to transport the signal from off equator to the equator.

Once the WNP heat content is modified, a key point is the displacement of heat content anomalies to the equatorial waveguide, a phase that was not discussed in previous studies. A first analysis suggests that the path taken by WNP heat content anomalies to reach the equatorial waveguide follows the complex currents pattern of the tropical northwest Pacific (Fig. 12). The WNP anomalies are first advected to the west by the North Equatorial Current (NEC; centered at 12°N); upon reaching the east coast of the Philippines, they are transported by the strong south-flowing western boundary current (or Mindanao Current; see Lukas et al. 1991) to about 5°N where they veer to the east. The anomalies are then advected by the North Equatorial Countercurrent (NECC) to the east and southeast to reach about 2°N near 140°E (Yu et al. 2000) where the southern edge of the NECC merges with the Equatorial Undercurrent (EUC) between depths of 100 and 200 m, to further feed the equatorial waveguide. This complex pattern may represent a strong challenge to the coarse global OGCM used here. However, the simulated patterns bear some resemblance to the observed currents and those modeled in higher-resolution GCMs (Matsumoto et al. 2001). In particular, the modeled currents and the associated transport reach their maximum in

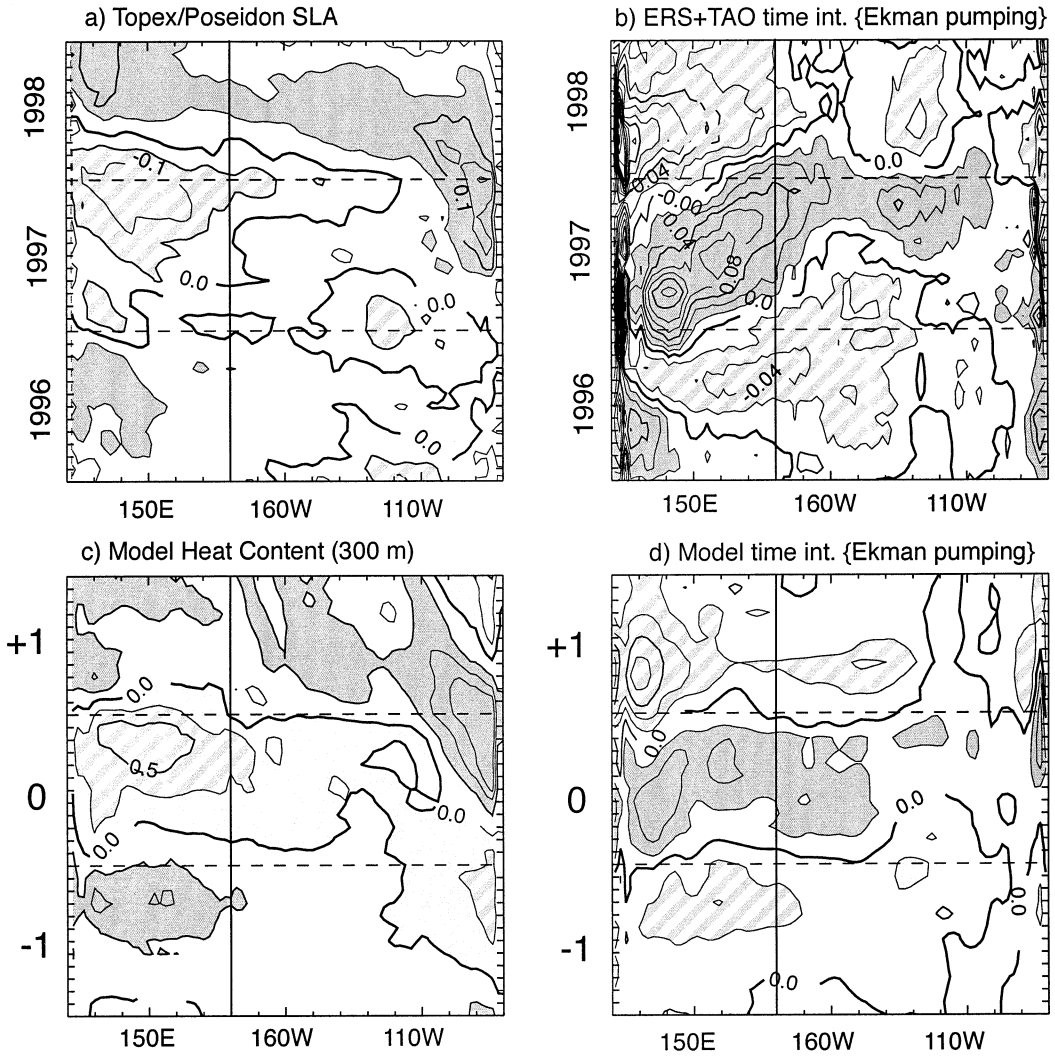

FIG. 10. Time–longitude diagram of (a),(c) heat content anomalies, and (b),(d) 6-month running time integral of wind stress curl meridionally averaged between 5° and 15°N. Observations (sea level anomaly from TOPEX/Poseidon and wind stress curl from ERS + TAO) are shown in (a) and (b). Coupled model ENSO composite values are shown in (c) and (d).

northern winter [between 0.5 and 1 m s^{-1} and a corresponding 20–30 Sv (1 Sv $\equiv 10^6$ m^3 s^{-1}) for both the Mindanao Current and the NECC—Fig. 12] like in observations. The fact that both positive and negative heat content anomalies are transported supports the fact that the mean currents (rather than the transients) are responsible for this advection. They allow for a rapid and efficient transit from the off-equatorial WNP region to the equator, between November and January (Figs. 11b,d). Northern winter therefore appears as a key season for communication between the northern Tropics and the equatorial waveguide.

b. El Niño onset

After describing the warm to cold ENSO turnabout, Wang et al. (1999) (and several other studies including Li 1997) argue that the warming is initiated by the same series of processes but with the opposite anomalies. According to the negative feedback loop discussed above, this would require cold SSTs in the eastern Pacific before every single El Niño event. An analysis of the observed Niño-3 SST anomaly time series shows that this happens often [composites of observed ENSO exhibit such a behavior; see, e.g., Fig. 3 of Torrence and Webster (1999)] but not always (as in 1981; Fig. 4). Moreover, the intensity of the east Pacific cooling does not seem to be directly related to the intensity of the following El Niño event (Fig. 4). The feedback loop discussed above (but with reverse patterns of sea level and winds) is only faintly visible in the 1997/98 El Niño onset (Fig. 11).

In the model composite, there is a clear systematic cooling in the eastern Pacific in the year before (year

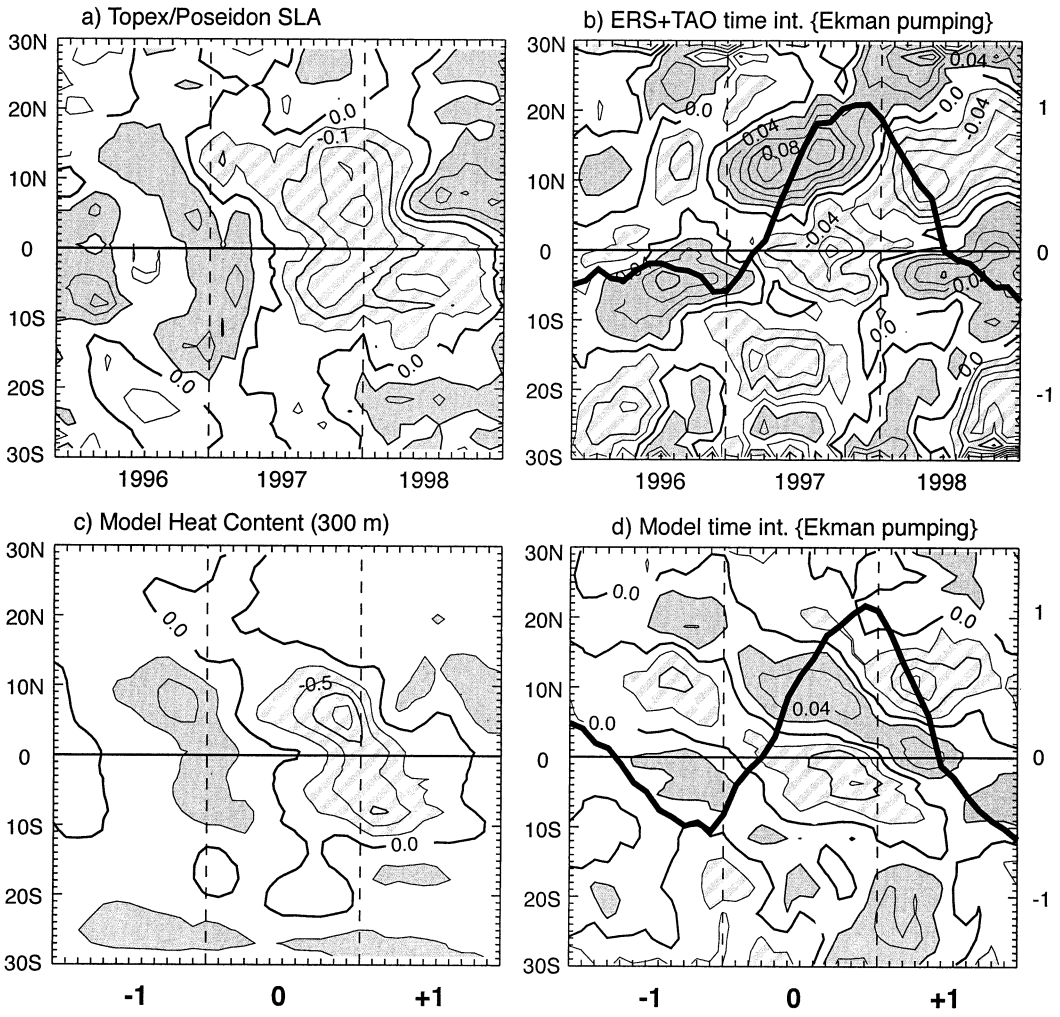

FIG. 11. Time–latitude diagram of (a),(c) heat content anomalies and (b),(d) 6-month running time integral of wind stress curl zonally averaged in the western Pacific between 120° and 170°E. The curves in (b),(d) are the Niño-3 SST anomalies (normalized by their respective maximum SSTs and multiplied by 20). Observations (sea level anomaly from TOPEX/Poseidon and wind stress curl from ERS + TAO) are shown in (a) and (b). Coupled model ENSO composite values are shown in (c) and (d).

−1 in Figs. 7d and 11d), and the patterns for the warm phase onset in the year before are very similar to the ones described for the decay phase, but of opposite signs. Here, the ENSO behavior seems to involve more systematically the reverse negative feedback loop (for El Niño onset) than in observations, the decay of a warm event very often leading to cold conditions in the eastern Pacific, which in turn trigger the onset of a new warm event (as for model years 95–100 in Fig. 4). This most likely explains the too strong 2-yr peak in modeled ENSO variability (Fig. 5). This bias can therefore be attributed to the too strong Walker circulation, which isolates the WNP region from other remote influences. Other studies using the same AGCM but different OGCMs exhibit the same bias [like Bacher et al. (1998) who found a 28-month peak variability and strong trade winds]. A simulation identical to the one used in the present study but using a T42 version of ECHAM4 both exhibits a weaker Walker circulation and a lower-frequency ENSO (2.8-yr instead of 2-yr peak; Gualdi et al. 2002b). These studies strongly suggest that the stronger-than-observed Walker circulation is responsible for the higher-than-observed ENSO frequency in agreement with the findings of Federov and Philander (2000). In reality, the local WNP heat content changes, which are forced by large-scale wind patterns, can have other remote origins, as for instance an anomalous monsoon in the year prior to a warm Pacific event (Krishnamurthy and Goswami 2000; Kim and Lau 2001).

c. The model aborted ENSO composite

Besides exhibiting weaker equatorial SST anomalies than the regular ENSO composite, the aborted ENSO

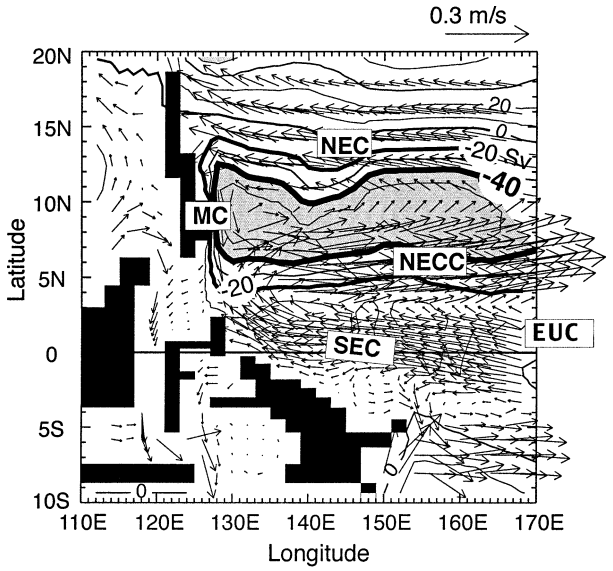

FIG. 12. Mean barotropic streamfunction in the west Pacific in Dec (shading) and associated modeled currents averaged in the first 200 m (arrows).

(ABORT) composite time structure is shifted by 6 months, the peak warming occurring in May (Fig. 13a). Subsurface equatorial structures also show eastward propagation, but they originate in the central Pacific (between 180° and 140°W) rather than in the western Pacific (Fig. 13b). A time–latitude section of the heat content anomaly in the central Pacific zonally averaged between the date line and 140°W also exhibits off-equator initiation of anomalies and subsequent equatorward propagation (Fig. 13a). This time though, the anomaly is located in the Southern Hemisphere. As the SST warms in the eastern Pacific, the atmospheric Gill's response (Fig. 13b) generates an anomalous cyclonic circulation which drives a strong anomalous Ekman pumping around 10°S during the first months of year 0 (Fig. 13a). At the same time, the SCZ is strong (Southern Hemisphere summer) and the associated westerlies (Figs. 2 and 14) drive an Ekman drift toward the equator. The off-equator cold anomalies are transferred to the equator in a month or two. Upon reaching the equatorial waveguide, the cooling propagates eastward during the second part of year 0 and the first months of year +1 (Fig. 13b), leading to cold SSTs in the eastern Pacific (Fig. 13a). A similar mechanism was proposed by Zhang and Rothstein (2000) to explain an equatorward transport of heat prior to the 1992 El Niño event, the sequence of events now occurring north of the equator (but still in the central Pacific) and the associated heat content anomalies being of the opposite sign.

In the ABORT case, the cooling of the east Pacific is very rapid when compared to the regular ENSO case. Indeed, the negative feedback loop does not involve a transit through the western Pacific current system, and does not allow for a full development of SST anomalies (the negative feedback loop lasting less than 6–8 months against one year for the regular ENSO). The initiation of the warming in year −1 also seems to be due to warm off-equator conditions (Fig. 13a) and equatorward Ekman transport due to the spurious westerlies at 10°S in the central Pacific from December to March (Figs. 2 and 14). The southern off-equator region was also in a warm state in 1992/93 when the unusual 1993 warming occurred (Goddard and Graham 1997), also reaching its peak value in spring (Fig. 4a). The persistent warm SST in the western and central Pacific also led to westerly anomalies in the south-central Pacific (Fig. 14). Goddard and Graham (1997) discussed this puzzling 1993 ''rewarming'' in the light of equatorial dynamics but could not come with a mechanism to explain it. The common features exhibited by the ABORT composite and the 1993 warming event suggest that off-equator processes may have been dominant.

The negative feedback mechanism discussed for the decay of the regular ENSO events in the Northern Hemisphere also applies in the Southern Hemisphere for the decay of the ABORT events, but with a 6-month shift. This suggests a strong role for the annual cycle, as this negative feedback favors the summer hemisphere, when the Gill's response is the strongest. The description of the ABORT composite further suggests a coherent relation of two model biases: the too strong and too zonal southern convergence zone and the too frequent ABORT events.

5. Summary and discussion

In this study, we explored the mechanisms leading to El Niño onset and termination in the ECHAM4/OPA (SINTEX) coupled ocean–atmosphere GCM. The modeled El Niño composites are validated against the well-observed 1997/98 El Niño event. They show quite good agreement on the various space and time structures associated with El Niño evolution both in the Pacific equatorial waveguide and off equator. This performance of the model is all the more important as very few fully coupled GCMs correctly simulate the mean state, the seasonal cycle, and the interannual variability in the tropical Pacific all together and without flux corrections. The analysis of the processes involved in ENSO phase change suggests that the model supports the basic mechanisms proposed by the various ENSO paradigms, while proposing additional features.

a. West Pacific role

The west Pacific heat content is confirmed as a precursor to ENSO phase change. Together with other studies (Wang et al. 1999), the present work emphasizes the role of its northern off-equator part (WNP region; 5°–15°N, 120°–170°E). The associated heat content changes appear to be dominated by a local Ekman pumping (or forced Rossby waves) rather than the accumulation of

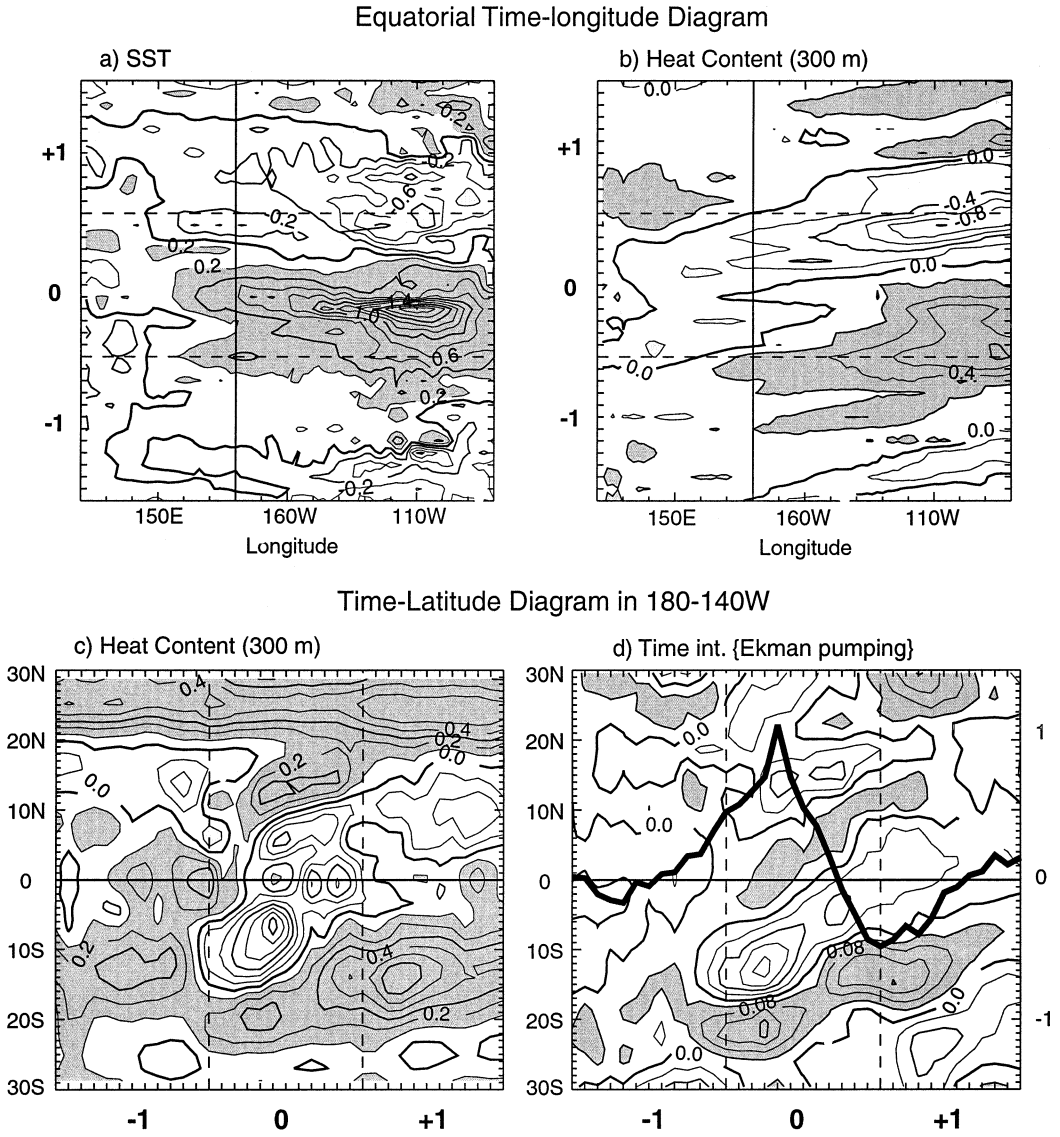

FIG. 13. Hovmoeller diagrams of monthly equatorial anomalies for the coupled model ABORT composite. (a),(b) Time–longitude diagrams at the equator for SST and heat content, respectively. (c),(d) Time–latitude diagrams of heat content anomalies and 6-month running time integral of wind stress curl zonally averaged in the central Pacific between 180° and 140°W. The curve in (d) is the composite Niño-3 SST anomaly.

remotely generated free Rossby waves. The absence of free Rossby waves propagating from the east has been a feature of very few ENSO theories, and supports the idea that the eastern boundary is not central to ENSO phase change (Schopf and Suarez 1990; Weisberg and Wang 1997).

b. ENSO phase change

El Niño termination in the model is due to a robust negative large-scale feedback loop in agreement with most paradigms (Fig. 15): as the SST rises in the eastern Pacific, the atmospheric Gill's response generates an anomalous cyclonic circulation over the WNP; the time integral of the corresponding upwelling over several months (forced Rossby wave) generates a reduced ocean heat content, which is then transported eastward by Kelvin waves that eventually lead to SST cooling in the eastern Pacific. This loop takes a year to be completed (from spring to spring), in agreement with the observed duration of most El Niño events. The time integral discussed here (from about June to December the year prior to the change) is explicitly set as the ''delay'' of the delayed oscillator paradigm, while it is implicit in the west Pacific oscillator. El Niño onset involves a similar mechanism, but with opposite signs, starting from an anomalous anticyclonic circulation in the WNP. The associated atmospheric circulation anomalies can also re-

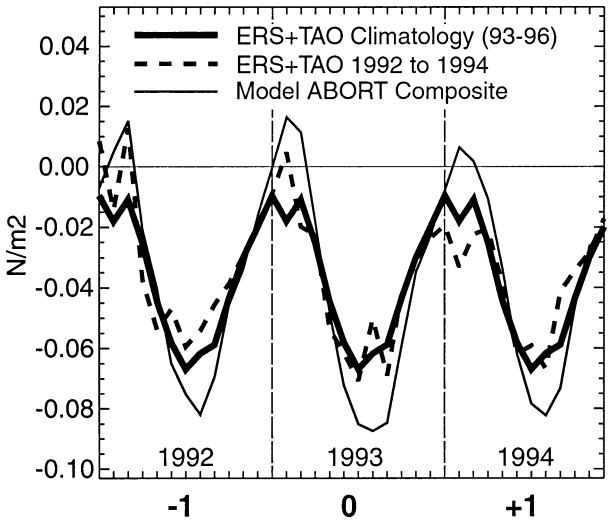

FIG. 14. Time series of zonal wind stress averaged in the south-central Pacific (5°–15°S, 180°–140°W). Thick solid line is the ERS + TAO climatology (repeated 3 times). Thin solid line is the coupled model ABORT composite. Dashed line is the ERS + TAO from Jan 1992 to Dec 1994.

sult from a Gill's response, requiring relatively cold SSTs in the eastern Pacific during the last 6–8 months of the year preceding the warming. Nevertheless, other remote atmospheric influences can modify the ocean heat content in the WNP (monsoon, intraseasonal oscillations, etc.). For instance, Torrence and Webster (1999) and Kirtman and Shukla (2000) noted a relation between the strong seasonal cycle in the tropical Pacific and both low ENSO variability and weak monsoon–ENSO relationships. Our results suggest that this relation is due to the change of influence of the Walker circulation: a strong seasonal cycle will favor a strong Walker circulation that will dominate over monsoon influences in the WNP region (Krishnamurthy and Goswani 2000; Lau and Wu 2001). This asymmetry between El Niño rise and El Niño decay, supported by the asymmetry between ''cold''[2] phases and warm phases of ENSO, suggests that an event is not directly produced by the previous extreme (and opposing) event as proposed by several theories. In other words, if ENSO is an oscillation, the physics of ''oscillation'' is probably more complex than what has been proposed from conceptual models, which only involve processes local to the tropical Pacific (this ''nonlinear'' argument was already noted by Schopf and Suarez 1988).

c. Off-equator to equator transport

The present study introduces the advection of the off-equator signal to the equatorial waveguide by the mean currents of western Pacific as an additional process. The associated delay is about 2 months. This point is in keeping with Cane and Sarachick's (1977) view of creating some western boundary current that has the net effect of transferring mass to the equator. Nevertheless, the off-equator to equator transport of heat content anomalies can take other routes: Ekman transport due to tropical westerlies (more likely to occur in winter, when the zonal winds are strong), and meridional ''draining'' at depth due to the strength of the surface convergence zones (Vintzileos et al. 1999); more likely to occur in summer). Further studies are needed to assess their relative roles in the mechanism proposed here.

d. Seasonality

Most of the processes described here seem to favor a particular season, supporting Wang's (1994) claim that the annual cycle and the ENSO cycle and strongly coupled (ENSO seasonal phase lock). The Gill's response to equatorial SST changes, central to ENSO phase change, is stronger in the summer hemisphere. The symmetrization of the circulation on either side of the equator that occurs in the model therefore favors two preferred times for tropical warming/cooling during the annual cycle (ENSO and ABORT events). In reality, the asymmetry of the seasonal cycle (in particular in the west, where the Australian continent occupies the Southern Hemisphere) can only favor the boreal winter warming, that is, what is known as El Niño. This can explain the results of Li (1997) who found in a simple model that his SST mode was destabilized from June to December and stabilized earlier in the year. Accordingly, when the southern Tropics are warm, the system becomes more symmetric and this can generate an equatorial warming in the Niño-3 region, but with a 6-month shift (like in the model ABORT events or in 1993). Hence, the El Niño seasonal phase lock can be viewed as a seasonal selection of processes. In an annual mean sense, these processes can appear as competing. This is the case in many theories, usually based on ENSO anomaly models, where the seasonal cycle is imposed and therefore not discussed. The west Pacific heat content buildup is stronger in northern summer/autumn, when the Gill's response is strongest. Northern winter is the preferred season for communication between the northern Tropics and the equatorial waveguide. The end of northern winter and the beginning of spring, when the trade winds/ocean surface currents relax, is the preferred season for Kelvin wave propagation to the east and favors an increased warming in the east Pacific (upwelling reduced). All these process occur during the seasonal cycle (regardless of the phase of ENSO) and their amplification (or damping) at the right moment can either trigger an El Niño event or its decay. The ENSO ''spring predictability barrier'' occurs when the trade winds relax in the east and central Pacific, allowing other processes, of secondary importance during the rest

[2] These cold phases, often referred to as ''La Niña,'' are in fact not statistically different from the normal state (J. Shukla 2002, personal communication).

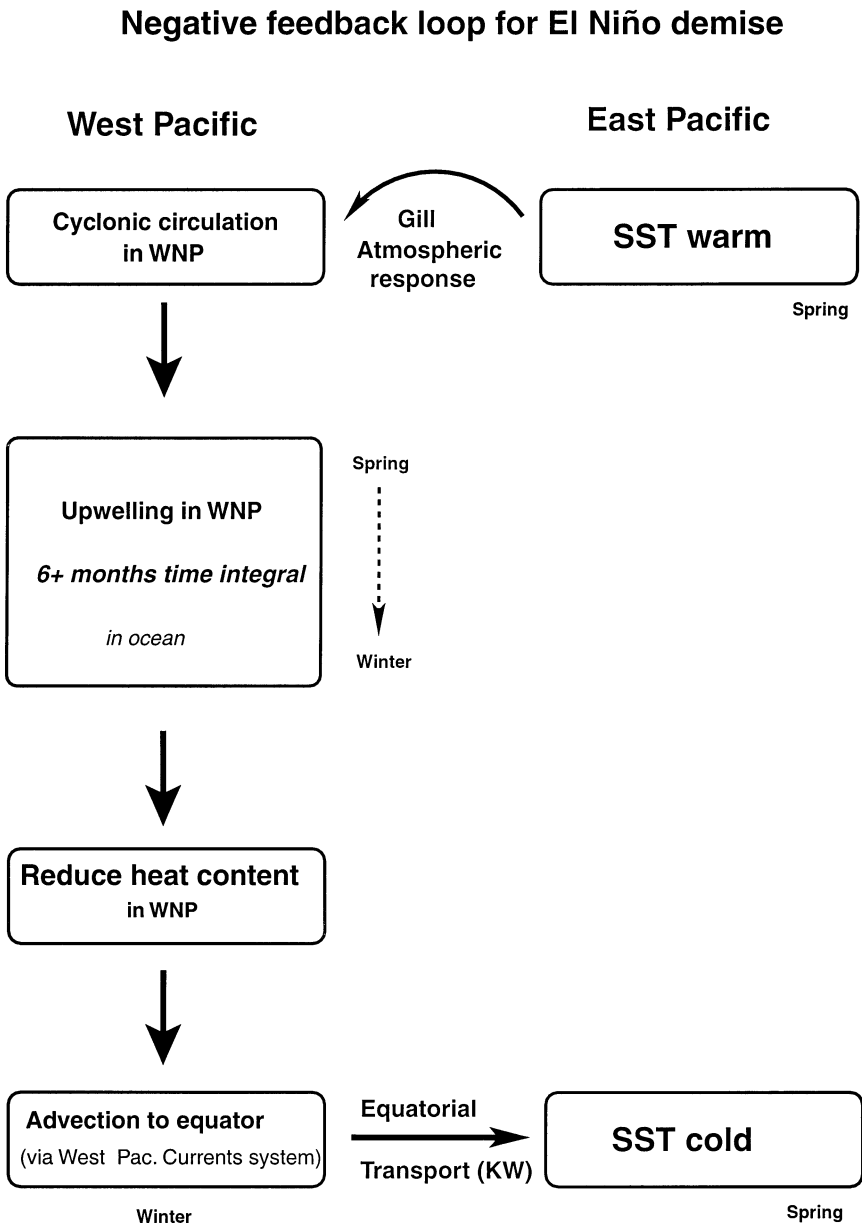

FIG. 15. Schematic diagram of the proposed negative feedback loop leading to ENSO phase change.

of the year, to play a role (like intraseasonal variability). In the model, the trade winds do not weaken in spring favoring a very regular and predictable ENSO (biennial oscillations).

e. Understanding model biases

The negative feedback loop described here suggests coherent relations between model biases. First, the stronger-than-observed modeled Walker circulation isolates the WNP from other remote influences, and leads to the strong biennial ENSO behavior (cold leading to warm and warm leading to cold) seen in the model (Fig. 5). The model also develops a spurious aborted ENSO composite: its structure resembles the regular ENSO composite but with smaller amplitude, a 6-month shift in timing (SST peak in May) and is restricted to the central and eastern Pacific. This bias appears to be related to the spurious existence of a southern convergence zone (SCZ) at 10°S in the central and eastern Pacific. Warm off-equator conditions permitting, the spurious westerlies associated with this SCZ drive the heat to the equatorial waveguide, triggering an east Pacific warming. The negative feedback loop of Fig. 15 efficiently acts to terminate the event, also through off-equator local Ekman pumping, this time located south

of the equator (10°S). This coherently links two biases of the coupled model: the SCZ and frequent aborted ENSO type. It is also shown that this aborted ENSO has similarities with the unusual 1993 spring warming. More generally, warm off-equator conditions associated with westerlies (like in the early 1990s) can efficiently drive heat toward the equatorial waveguide (Zhang and Rothsein 2000).

The many ENSO features exhibited by the present SINTEX model makes it a good tool to further investigate the mechanisms of tropical variability. For instance, a more detailed analysis of ocean and atmosphere transients could provide a clearer discrimination between the different ENSO paradigms. An analysis of the impact of intraseasonal variability (well reproduced by the model) on ENSO can also shed light on the irregularity and diversity of El Niño events. The link with the monsoon and a possible two-way coupling with ENSO is discussed in further detail in Gualdi et al. (2002a). The model exhibits some ENSO decadal variability. The possible relation with the variations of the mean state, as proposed by several studies will be investigated in a future paper.

Acknowledgments. We wish to thank Gurvan Madec, Jean-Philippe Boulanger, and Julia Slingo for helpful discussions. This work was mostly funded by the SINTEX EU Contract ENV4-CT 98-0714. Computations were carried on the SINTEX NEC-SX4 and the postprocessing was done at the IDRIS centre of CNRS. We wish to thank Pascal Terray for computing the confidence intervals of the model composites, Bill Kessler for providing his tropical Pacific ocean analysis, Nick Rayner for providing the HadISST1 dataset, the TOPEX/Poseidon program, and Pauline Schnapper for improving the English of this paper.

REFERENCES

AchutaRao, K., and K. R. Sperber, 2002: Simulation of the El Niño–Southern Oscillation: Results from the coupled model intercomparison project. *Climate Dyn.,* **19,** 191–209.

Bacher, A., J. M. Oberhuber, and E. Roeckner, 1998: ENSO dynamics and seasonal cycle in the tropical Pacific as simulated by the ECHAM4/OPYC3 coupled general circulation model. *Climate Dyn.,* **14,** 431–450.

Barthelet, P., L. Terray, and S. Valcke, 1998: Transient CO_2 experiment using the ARPEGE/OPAICE non-flux corrected coupled model. *Geophys. Res. Lett.,* **25,** 2277–2280.

Battisti, D. S., and A. C. Hirst, 1989: Interannual variability in the tropical atmosphere–ocean system: Influence of the basic state and ocean geometry. *J. Atmos. Sci.,* **46,** 1678–1712.

Bjerknes, J., 1969: Atmospheric teleconections from the equatorial Pacific. *Mon. Wea. Rev.,* **97,** 163–172.

Blanke, B., and P. Delecluse, 1993: Low-frequency variability of the tropical Atlantic Ocean simulated by a general circulation model with mixed layer physics. *J. Phys. Oceanogr.,* **23,** 1363–1388.

Boulanger, J. P., and Coauthors, 2001: Role of non-linear ocean processes to westerly wind events: New implications for the 1997 El Niño onset. *Geophys. Res. Lett.,* **28,** 1603–1606.

Braconnot, P., S. Joussaume, O. Marti, and N. de Noblet, 1999: Synergistic feedback from ocean and vegetation on the African monsoon response to mid-Holocene insolation. *Geophys. Res. Lett.,* **26,** 2481–2484.

Cane, M. A., and E. S. Sarachick, 1977: Forced baroclinic ocean motions: II: The linear equatorial bounded case. *J. Mar. Res.,* **35,** 395–432.

Cassou, C., and C. Perigaud, 2000: ENSO simulated by intermediate coupled models and evaluated with observations over 1970–98. Part II: Role of the off-equatorial ocean and meridional winds. *J. Climate,* **13,** 1635–1663.

Collins, M., 2000: The El Niño–Southern Oscillation in the second Hadley Centre coupled model and its response to greenhouse warming. *J. Climate,* **13,** 1299–1312.

Covey, C., and Coauthors, 2000: The seasonal cycle in coupled ocean–atmosphere general circulation models. *Climate Dyn.,* **16,** 775–787.

Delecluse, P., M. Davey, Y. Kitamura, S. Philander, M. Suarez, and L. Bengtsson, 1998: TOGA review paper: Coupled general circulation modeling of the tropical Pacific. *J. Geophys. Res.,* **103,** 14 357–14 373.

Fedorov, A. V., and S. G. Philander, 2000: Is El Niño changing? *Science,* **288,** 1997–2002.

Friedlingstein, P., L. Bopp, P. Ciais, J.-L. Dufresne, L. Fairhead, H. LeTreut, P. Monfray, and O. Aumont, 2001: On the positive feedback between the climate system and the carbon cycle under the anthropogenic perturbation. *Geophys. Res. Lett.,* **28,** 1543–1546.

Gill, A. E., 1980: Some simple solution of heat-induced tropical. *Quart. J. Roy. Meteor. Soc.,* **106,** 447–462.

Goddard, L., and N. E. Graham, 1997: El Niño in the 1990s. *J. Geophys. Res.,* **102,** 10 423–10 436.

Graham, N. E., and W. B. White, 1991: Comments on ''on the role of off-equatorial oceanic Rossby waves during ENSO.'' *J. Phys. Oceanogr.,* **21,** 453–460.

Gualdi, S., E. Guilyardi, A. Navarra, S. Masina, and P. Delecluse, 2002a: The interannual variability in the tropical Indian Ocean as simulated by a coupled GCM. *Climate Dyn.,* in press.

——, A. Navarra, E. Guilyardi, and P. Delecluse, 2002b: The sintex coupled GCM. The tropical Indo-Pacific region. *Ann. Geofis.,* in press.

Guilyardi, E., and G. Madec, 1997: Performance of the OPA/ARPEGE-t21 global ocean–atmosphere coupled model. *Climate Dyn.,* **13,** 149–165.

——, ——, and L. Terray, 2001: The role of lateral ocean physics in the upper ocean thermal balance of a coupled ocean–atmosphere GCM. *Climate Dyn.,* **17,** 589–599.

Inness, P., J. Slingo, E. Guilyardi, and J. Cole, 2003: Simulation of the Madden–Julian oscillation in a coupled general circulation model. Part II: The role of the basic state. *J. Climate,* **16,** 365–382.

Ji, M., A. Leetmaa, and J. Derber, 1995: An ocean analysis system for seasonal to interannual climate studies. *Mon. Wea. Rev.,* **123,** 460–481.

Jin, F.-F., 1997a: An equatorial ocean recharge paradigm for ENSO. Part I: Conceptual model. *J. Atmos. Sci.,* **54,** 811–829.

——, 1997b: An equatorial ocean recharge paradigm for ENSO. Part II: A stripped-down coupled model. *J. Atmos. Sci.,* **54,** 830–847.

——, and S.-I. An, 1999: Thermocline and zonal advective feedbacks within the equatorial ocean recharge oscillator model for ENSO. *Geophys. Res. Lett.,* **26,** 2989–2992.

Kessler, W. S., and J. McCreary, 1993: The annual wind-driven Rossby wave in the subthermocline equatorial Pacific. *J. Phys. Oceanogr.,* **23,** 1192–1207.

Kim, K.-M., and K.-M. Lau, 2001: Dynamics of monsoon-induced biennial variability in ENSO. *Geophys. Res. Lett.,* **28,** 315–318.

Kirtman, B., and J. Shukla, 2000: Influence of the Indian summer monsoon on ENSO. *Quart. J. Roy. Meteor. Soc.,* **126,** 213–239.

Krishnamurthy, V., and B. N. Goswami, 2000: Indian monsoon–ENSO relationship on interdecadal timescale. *J. Climate,* **13,** 579–595.

Latif, M., and Coauthors, 2001: ENSIP: The El Niño simulation intercomparison project. *Climate Dyn.,* **18,** 255–276.

Lau, K.-M., and H. T. Wu, 2001: Principal modes of rainfall–SST variability of the Asian summer monsoon: A reassessment of the monsoon–ENSO relationship. *J. Climate,* **14,** 2880–2895.

Levitus, S., 1982: *Climatological Atlas of the World Ocean.* NOAA Prof. Paper 13, 173 pp. and 17 microfiche.

—— and T. P. Boyer, 1994: *Temperature.* Vol. 4, *World Ocean Atlas 1994,* NOAA Atlas NESDIS 4, 117 pp.

Li, T., 1997: Phase transition of the El Niño–Southern Oscillation: A stationary SST mode. *J. Atmos. Sci.,* **54,** 2872–2887.

Lukas, R., E. Firing, P. Hacker, P. L. Richardson, C. A. Collins, R. Fine, and R. Gammon, 1991: Observations of the Mindanao Current during the western equatorial Pacific Ocean circulation study. *J. Geophys. Res.,* **96,** 7089–7104.

Madec, G., P. Delecluse, M. Imbard, and C. Levy, 1998: OPA version 8.1 ocean general circulation model reference manual. Tech. Rep. LODYC/IPSL Note 11, 91 pp.

Matsumoto, Y., T. Kagimoto, M. Yoshida, M. Fukuda, N. Hirose, and T. Yamagata, 2001: Intraseasonal eddies in the Sulawesi Sea simulated in an ocean general. *Geophys. Res. Lett.,* **28,** 1631–1634.

McPhaden, M., 1999: Genesis and evolution of the 1997–1998 El Niño. *Science,* **283,** 950–954.

Mechoso, C. R., and Coauthors, 1995: The seasonal cycle over the tropical Pacific in coupled ocean–atmosphere general circulation models. *Mon. Wea. Rev.,* **123,** 2825–2838.

Meehl, G. A., and J. M. Arblaster, 1998: The Asian–Australian monsoon and El Niño–Southern Oscillation in the NCAR climate system model. *J. Climate,* **11,** 1356–1385.

Meinen, C. S., and M. J. McPhaden, 2001: Interannual variability in warm water volume transports in the equatorial Pacific during 1993–99. *J. Phys. Oceanogr.,* **31,** 1324–1345.

Menkes, C., J.-P. Boulanger, A. J. Busalacchi, J. Vialard, P. Delecluse, M. J. McPhaden, E. Hackert, and N. Grima, 1998: Impact of TAO vs. ERS wind stresses onto simulations of the tropical Pacific Ocean during the 1993–1998 period by the OPA OGCM. *Climatic Impact of Scale Interaction for the Tropical Ocean–Atmosphere System—Euroclivar Workshop No. 13,* J. Slingo and P. Delecluse, Eds., Euroclivar, 46–48.

Mocrette, J. J., 1991: Radiation and cloud radiative properties in the European Centre for Medium-Range Weather Forecasts forecasting system. *J. Geophys. Res.,* **96,** 9121–9132.

Neelin, J. D., D. Battisti, A. Hirst, F.-F. Jin, Y. Wakata, T. Yamagata, and S. Zebiak, 1998: ENSO theory. *J. Geophys. Res.,* **103,** 14 261–14 290.

Nordeng, T. E., 1994: Extended versions of the convective parameterization scheme at ECMWF and their impact on the mean and transient activity of the model in the Tropics. ECMWF Tech. Memo. 206, ECMWF Research Dept., European Center for Medium-Range Weather Forecasts, Reading, United Kingdom, 25 pp.

Perigaud, C., F. Melin, and C. Cassou, 2000: ENSO simulated by intermediate coupled models and evaluated with observations over 1970–98. Part I: Role of the off-equatorial variability. *J. Climate,* **13,** 1605–1634.

Picaut, J., M. Ioualalen, C. Menkes, T. Delcroix, and M. McPhaden, 1996: Mechanism of the zonal displacements of the Pacific warm pool, implications for ENSO. *Science,* **274,** 1486–1489.

Rasch, P. J., and D. L. Williamson, 1990: Computational aspects of moisture transport in global models of the atmosphere. *Quart. J. Roy. Meteor. Soc.,* **116,** 1071–1090.

Rasmusson, E. M., and T. H. Carpenter, 1982: Variations in tropical sea surface temperature and surface wind fields associated with the Southern Oscillation/El Niño. *Mon. Wea. Rev.,* **110,** 354–384.

Raynaud, S., S. Speich, E. Guilyardi, and G. Madec, 2000: Impacts of the ocean lateral diffusion on the El Niño/Southern Oscillation–like variability of a global coupled general circulation model. *Geophys. Res. Lett.,* **27,** 3041–3044.

Roeckner, E., and Coauthors, 1996: The atmospheric general circulation model ECHAM-4: Model description and simulation of present-day climate. Max-Planck-Institut für Meteorologie Rep. 218, 94 pp.

Schneider, N., S. Venzke, A. J. Miller, D. W. Pierce, T. P. Barnett, C. Deser, and M. Latif, 1999: Pacific thermocline bridge revisited. *Geophys. Res. Lett.,* **26,** 1329–1332.

Schopf, P. S., and M. J. Suarez, 1988: Vacillations in a coupled ocean–atmosphere system. *J. Atmos. Sci.,* **45,** 549–566.

——, and ——, 1990: Ocean wave dynamics and the timescale of ENSO. *J. Phys. Oceanogr.,* **20,** 629–645.

Suarez, M. J., and P. S. Schopf, 1988: A delayed action oscillator for ENSO. *J. Atmos. Sci.,* **45,** 3283–3287.

Terray, L., 1998: Sensitivity of climate drift to atmospheric physical parameterizations in a coupled ocean–atmosphere general circulation model. *J. Climate,* **11,** 1633–1658.

Tiedtke, M., 1989: A comprehensive mass flux scheme for cumulus parametrization in large-scale models. *Mon. Wea. Rev.,* **117,** 1779–1800.

Torrence, C., and P. Webster, 1999: Interdecadal changes in the ENSO–monsoon system. *J. Climate,* **12,** 2679–2690.

Valcke, S., L. Terray, and A. Piacentini, 2000: The OASIS coupled user guide version 2.4. Tech. Rep. TR/CMGC/00-10, CERFACS, 85 pp.

Vialard, J., C. Menkes, J. Boulanger, E. Guilyardiand, P. Delecluse, and M. J. McPhaden, 2001: Oceanic mechanisms driving the SST during the 1997–98 El Niño. *J. Phys. Oceanogr.,* **31,** 1649–1675.

Vintzileos, A., P. Delecluse, and R. Sadourny, 1999: On the mechanisms in a tropical ocean–global atmosphere coupled general circulation model. Part II: Interannual variability and its relation to the seasonal cycle. *Climate Dyn.,* **15,** 63–80.

Wang, B., R. Wu, and R. Lukas, 1999: Roles of the western North Pacific wind variation in thermocline adjustment and ENSO phase transition. *J. Meteor. Soc. Japan,* **77,** 1–16.

Wang, C., 2001: A unified oscillator model for the El Niño–Southern Oscillation. *J. Climate,* **14,** 98–115.

Wang, X. L., 1994: The coupling of the annual cycle and ENSO over the tropical Pacific. *J. Atmos. Sci.,* **51,** 1115–1136.

Weisberg, R., and C. Wang, 1997: A western Pacific oscillator paradigm for the El Niño–Southern Oscillation. *Geophys. Res. Lett.,* **24,** 779–782.

White, W., G. Meyers, J.-R. Donguy, and S. Pazan, 1985: Short-term climatic variability and thermal structure of the Pacific Ocean during 1979–82. *J. Phys. Oceanogr.,* **15,** 917–935.

Wyrtki, K., 1975: El Niño—The dynamic response of the equatorial Pacific Ocean to atmospheric forcing. *J. Phys. Oceanogr.,* **5,** 572–584.

——, 1985: Water displacements in the Pacific and the genesis of El Niño cycles. *J. Geophys. Res.,* **90,** 7129–7132.

Yu, Z., J. P. McCreary, W. S. Kessler, and K. A. Kelly, 2000: Influence of equatorial dynamics on the Pacific north equatorial countercurrent. *J. Phys. Oceanogr.,* **30,** 3179–3190.

Zebiak, S. E., 1989: Ocean heat content variability and El Niño cycles. *J. Phys. Oceanogr.,* **19,** 475–486.

——, and M. A. Cane, 1987: A model El Niño–Southern Oscillation. *Mon. Wea. Rev.,* **115,** 2262–2278.

Zhang, R.-H., and S. Levitus, 1996: Structure and evolution of interannual variability of the tropical Pacific upper ocean temperature. *J. Geophys. Res.,* **101,** 20 501–20 524.

——, and L. M. Rothstein, 2000: Role of off-equatorial subsurface anomalies in initiating the 1991–1992 El Niño as revealed by the National Centers for Environmental Prediction ocean reanalysis data. *J. Geophys. Res.,* **105,** 6327–6340.

——, L. Rothstein, and A. Busalacchi, 1998: Origin of upper-ocean warming and El Niño change on decadal scales in the tropical Pacific Ocean. *Nature,* **391,** 879–883.